Precise 50 to 60 GHz Measurements on a Two-Mile Loop of Helix Waveguide

By D. T. YOUNG and W. D. WARTERS

Precise measurements made in the 50 GHz to 60 GHz band on a two-mile triangular loop of 2 inch diameter helix waveguide are presented. The measuring technique is discussed in some detail regarding accuracy. A brief comparison of the experimental results with theory is made. The average measured attenuation of the waveguide varies smoothly from 2.62 dB per mile at 50 GHz to 2.32 dB per mile at 60 GHz. Fast variations versus frequency were within experimental error. Several short-radius bends of different angles were measured; losses less than 0.8 dB across the band were observed for a 42° bend made of mitered elbows.

I. INTRODUCTION

Low-loss transmission via the TE_{01} mode in circular waveguide has been studied for many years for use as a wideband communication medium.[1] Much work has been done on the design of improved waveguides,[2, 3] the understanding of the effects of spurious modes,[4, 5] and the measurement of sample guides over wide frequency bands.[6, 7]

Interesting waveguide communication system layouts have proposed repeater spacings in the range of 10 to 20 miles. Reasonable design requires that the total loss of such a waveguide section be predictable to within a few dB. However, the longest guides on which measurements have been reported are a few hundred yards, and the variation to be expected between different samples of similar construction is unknown.

This paper describes measurements made in the 50 GHz to 60 GHz band on a two-mile triangular loop of helix waveguide. Extremely precise observations were made on many sections of the loop in order to:

(*i*) Test whether the loss of a long line is indeed the sum of the losses of its component sections as is expected if the sections act independently.

(*ii*) Discover the statistical variations between sections, both in average loss and loss fluctuations with frequency, so that confidence limits can be found for predicting the behavior of very long lines from measurements on shorter lines.
(*iii*) Allow accurate measurements of bends and other components by taking the difference between the losses of sections with and without the test component included.

II. THE TWO-MILE WAVEGUIDE LOOP

The two-mile facility was constructed at Holmdel, New Jersey, by A. C. Beck and C. F. P. Rose. The permanent installation consists of a triangular shaped loop of two parallel 4-inch steel conduits buried below the frost line, with poured concrete ties every 10 feet, along a precisely aligned path. The layout is shown in Fig. 1. The loop begins and ends in a laboratory building, and large waterproof access manholes are provided approximately every 400 feet, as indicated by the letters in Fig. 1. The waveguide was installed in the conduit by adding sections in one manhole and pulling the assembled guide through the conduit to the next manhole with a cable and winch.

The vertical profile of the path is quite smooth, with no radii of curvature less than 4,000 feet. The horizontal plan of the path consists of straight lines, as shown in Fig. 1, except the two sections between manholes U, V, and W. These sections have a constant radius of curvature of 708 feet. The angles at the corners of the loop are 90°, 90°, and 42°.

The waveguide was two-inch inside diameter steel-jacketed helix waveguide. It was constructed at the Holmdel Laboratory by A. C. Beck and C. F. P. Rose and has been described by them.[3] It was made in 15-foot lengths which were connected with precision threaded couplings. The guide rests on its couplings in the steel conduit between manholes, and is thus supported at 15-foot intervals. A short connecting section is provided in each manhole; it is easily removed to allow insertion of measuring gear.

The total added loss at 55 GHz owing to the horizontal and vertical path bends has been calculated by A. C. Beck to be 0.045 dB and 0.002 dB, respectively, for the whole two miles. The former was readily measured, the latter was beyond our measurement accuracy.

To complete the loop, various types of sharp-radius bends were placed in the corner manholes H, O, and U. Section IV describes these bends and experimental measurements on them.

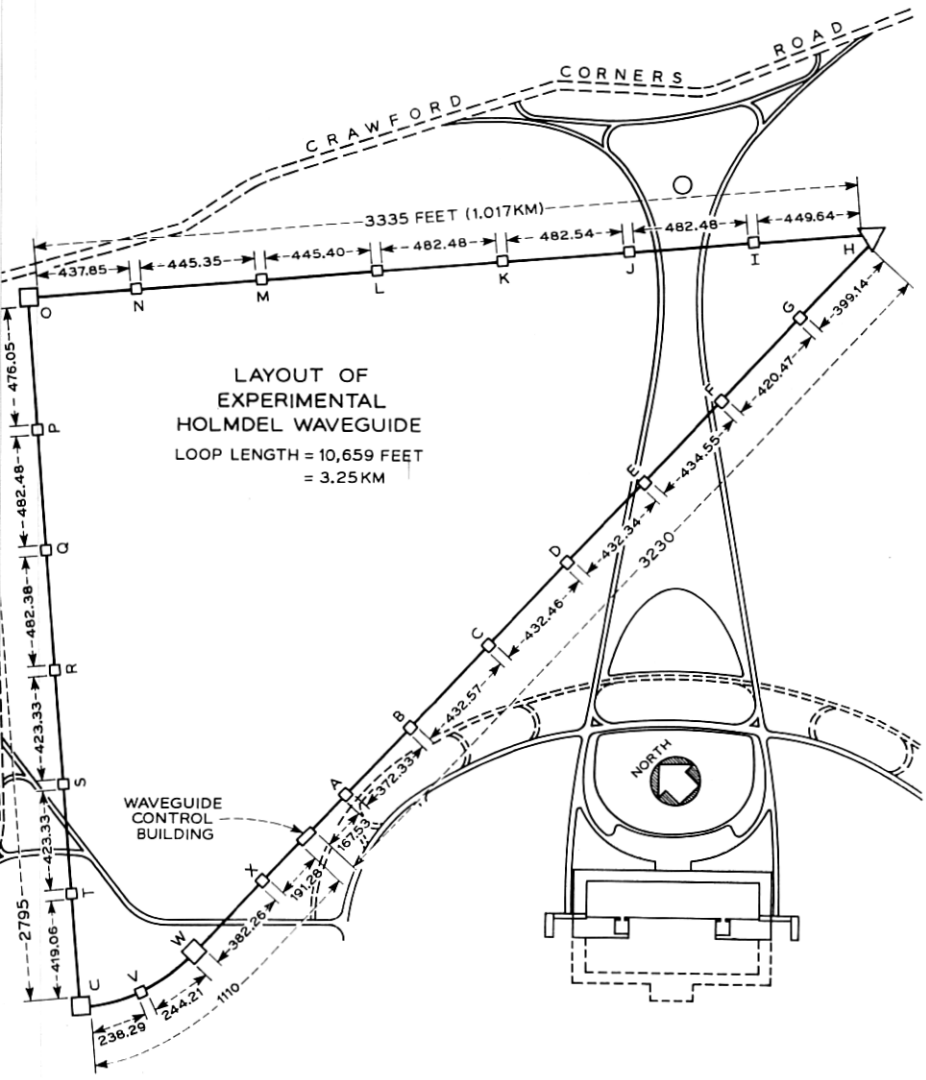

Fig. 1 — Layout of experimental Holmdel waveguide.

The entire waveguide loop, including bends, was made vacuum tight and could be evacuated to a pressure of a few microns of mercury. All measurements were made with the guide filled to slightly over one atmosphere with high purity dry nitrogen. Each time the guide was opened to change experimental conditions it was

flushed with nitrogen, pumped, then refilled. These precautions are necessary to eliminate oxygen, which has several strong absorption lines in our band of interest.

III. MEASURING TECHNIQUES AND DATA REDUCTION

The TE_{01} transmission losses of the waveguide sections of interest were measured by the shuttle-pulse method. This method allows highly accurate measurements on low-loss line sections, provided that certain precautions are observed, because it includes observations on many round-trip traversals of the section and because the time resolution of the pulse allows spurious reflections to be avoided.

3.1 *Apparatus*

Figure 2 is a block diagram of the measuring setup. It used a heterodyne receiver system in which the CW beating oscillator signal and the transmitted test pulses are both provided from a single backward wave oscillator by pulsing the beam voltage every 100 μs with a 0.1 μs duration pulse which changes the oscillator frequency by 70 MHz. This scheme was suggested by D. H. Ring and has been described earlier.[6] The test pulses and beating oscillator power driving the converter are reflected from the coupling mesh. A portion of each transmitted signal pulse enters the test section and bounces back and forth between the mesh and piston in the test section many times, thus causing a train of pulses with decreasing amplitudes to be returned to the receiver.

Since the mesh has transmission loss of approximately 17 dB, the level of the signal pulses which have traveled in the test section before returning to the converter is at least 34 dB below the beating oscillator level and good receiver linearity is assured. The transmitter power and receiver noise figure allowed as many as 100 trips to be observed, depending on the length of the test section.

The 70 MHz IF pulse train passes through a precision attenuator adjustable in 0.1 dB steps. The range unit opens a 0.4 μs time gate to select a desired pulse from the train. The selected pulse is peak-detected and read on an expanded-scale levelmeter. The attenuator is set to center the levelmeter, so the entire IF strip operates at constant level. Readings of relative pulse height may readily be made to within 0.05 dB. Measurements are made, after adjusting the BWO and converter for the desired frequency, by selecting a series of pulses (usually 15 to 20) from the train with the range unit and recording

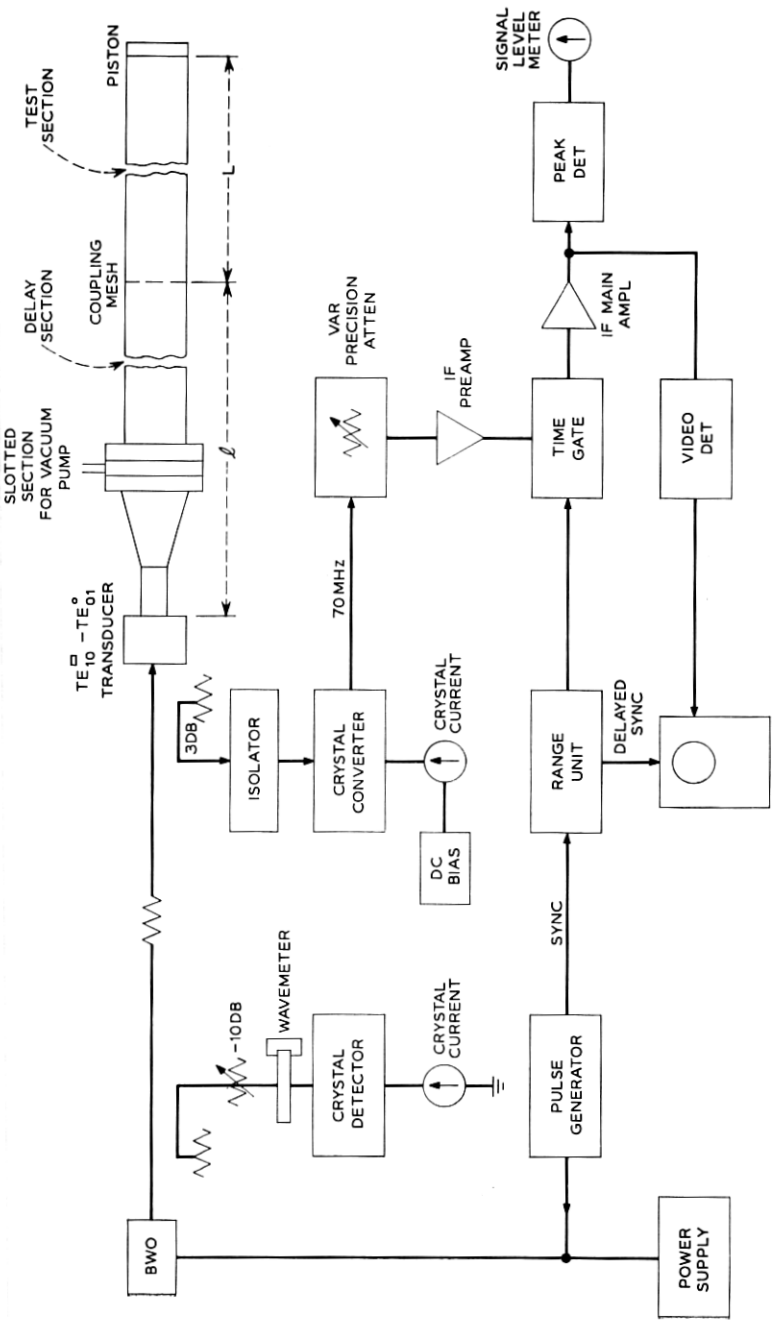

Fig. 2 — Block diagram of measuring setup.

the trip number and relative pulse height of each. This data, together with end corrections for mesh and piston return losses, is reduced by a simple computer program.

The millimeter-wave circuitry is all of precision construction and, with the exception of the $TE_{10}^{\square}$–TE_{01}° transducer, is extremely well matched. The effects of the 15 to 20 dB return loss of the transducer will be discussed later.

The coupling mesh is a flat transverse copper plate 1/32 inch thick with many small uniformly-spaced holes. Care was taken in machining both it and its mounting fixture to insure flatness. The shorting piston was ¼ inch thick solid copper, machined for flatness and polished. The return loss of the mesh was precisely measured by substituting it for the solid piston in a short test line (terminated beyond it) and comparing the relative pulse heights of the 100th trips in the two cases. The mesh return loss varies between 0.054 and 0.114 dB across the 50-60 GHz band. The return loss of the solid copper piston is taken to be the calculated value of 0.005 dB.

The shuttle pulse technique provided a further important advantage for the present experiments, where many sections physically separated by large distances were to be measured, by allowing the test gear to remain in one location. The coupling mesh to the test section was placed in any desired manhole around the loop, and the shorting piston for the far end of the test section was then placed in the appropriate following manhole.

The waveguide between the building where the test gear was located and the manhole where the coupling mesh was located served as a transmission line. Thus measurements could be made on the waveguide section between any two manholes chosen by the experimenter simply by locating the mesh and piston appropriately. The waveguide between the test gear and the coupling mesh also served as a delay line to allow complete time separation between the incident pulse and the pulse reflected from the mismatch at the mode transducer.

Unless these pulses are separated the effective return loss of the coupling mesh will vary considerably. The measured return loss of the coupling mesh is then no longer correct, and this will seriously affect the accuracy of measurement of short waveguides.

3.2 *Data Reduction*

The basic assumption in shuttle pulse measurements is that the loss of each successive trip through the test section is identical, thus

the total loss in decibels is a linear function of trip number. The validity of this assumption for our experiment is discussed in Section 3.3.

In order to obtain high precision, many sets of pulse height level vs trip number readings (h_i, n_i) were taken at each test frequency for each test line. To weight the readings equally and to obtain a measure of the experimental precision, a straight line was fitted by the method of least squares. Thus A and B were chosen such that $M(A, B)$ was minimized, where

$$M(A, B) = \sum_{i=1}^{N} (h_i - A + Bn_i)^2.$$

This requires

$$A = \frac{K \sum_{i=1}^{N} n_i h_i - Q \sum_{i=1}^{N} h_i}{K^2 - NQ}$$

$$B = \frac{N \sum_{i=1}^{N} n_i h_i - K \sum_{i=1}^{N} h_i}{K^2 - NQ}$$

where

$$K = \sum_{i=1}^{N} n_i$$

$$Q = \sum_{i=1}^{N} n_i^2$$

and N is the number of data pairs (h_i, n_i). B is therefore the desired experimental loss per trip and A is the intercept at zero trips. A depends upon the transmitter power level and is of interest mainly as an internal check that the data is consistent with other measurements. The attenuation constant α of the test section is then computed from

$$\alpha(f) = \frac{1}{2L} [B(f) - C(f)] \tag{1}$$

where L is the length of the section, B is the measured round trip loss and C is the known end correction.

If we assume that the pulse height measurements h_i are distributed normally about the true line $A_t - B_t n_i$, we can readily calculate the standard deviation of B, our experimental measure of B_t, and thus the accuracy of our experimental value of α.

If we assume the variance $\hat{\Delta}^2$ of the h_i is known so that

$$h_i = A_t - B_t n_i + \Delta_i \tag{2}$$

with $\langle \Delta_i \rangle = \langle \Delta_i \Delta_k \rangle = 0$, except $\langle \Delta_i^2 \rangle = \hat{\Delta}^2$, where $\langle\ \rangle$ is the statistical expected value, then we can readily calculate

$$\langle (B - B_t)^2 \rangle = \frac{N\hat{\Delta}^2}{NQ - K^2}. \tag{3}$$

Thus the accuracy of the experimentally determined loss is related to the individual measurement variance $\hat{\Delta}^2$ by equation (3).

If the variance $\hat{\Delta}^2$ is unknown then one can use the variable

$$t = (B - B_t)\sqrt{\frac{(N-2)(NQ - K^2)}{NM}} \tag{4}$$

where N, M, K and Q are as previously defined. It can be shown[8] that t has Student's t distribution with $N - 2$ degrees of freedom,

$$f(t) = \text{Const}\left(1 + \frac{t^2}{N-2}\right)^{-(N-1)/2}. \tag{5}$$

From (4) we can write

$$\langle (B - B_t)^2 \rangle = \frac{NM}{(N-2)(NQ - K^2)} \langle t^2 \rangle$$

and $\langle t^2 \rangle$ can be evaluated from (5) to give

$$\langle (B - B_t)^2 \rangle = \frac{NM}{(N-4)(NQ - K^2)}, \qquad N > 4. \tag{6}$$

The value of $\langle (B - B_t)^2 \rangle$ was calculated from (6) for each measurement. Comparison with (3) over many measurements gives a value for $\hat{\Delta}$ of about 0.05 dB, which is in agreement with the expected limit of accuracy of our pulse height measurements.

The loss in dB per mile as calculated from (1) and the standard deviation of the measurement as calculated from (6) were plotted versus frequency for each test section by the computer. Some of these results are shown in Figs. 3 to 8 and are discussed in detail in Section 4.

For most test sections, measurements were made at frequencies spaced by 100 MHz from 50 to 51 GHz and from 59 to 60 GHz, and at frequencies spaced by 1 GHz from 51 to 59 GHz. This arrangement allowed a check at the ends of the band on the consistency between the calculated deviations and the actual spread of points, and gave sufficiently fine-grained data across the band to detect any expected

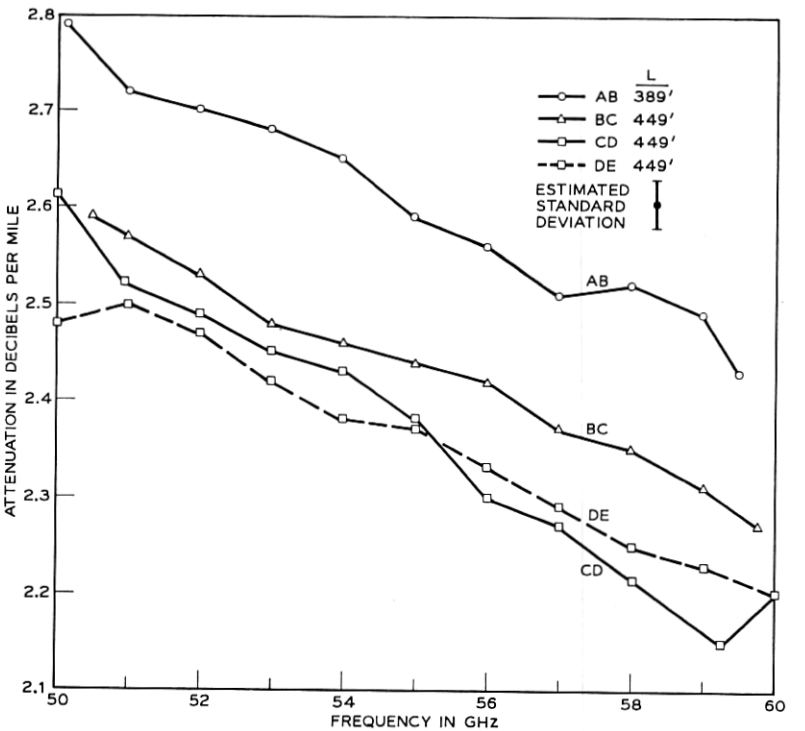

Fig. 3 — Measured attenuation of short length waveguide sections.

variations with frequency. Helix waveguide of the type used in these experiments is not expected to show loss variations vs frequency with periods less than 6 GHz.[9]

3.3 *Experimental Precautions and Limitations*

There are a variety of precautions that must be observed in shuttle pulse measurements in order to avoid anomalies and inaccuracies.

Of prime importance for high precision is that there be no interaction between different traversals of the signal pulse in the test section. Otherwise the observed loss will not be a linear function of the number of trips and the desired single trip loss will be difficult to derive. Interactions can occur in two major ways: (*i*) between successive trips when spurious mode generation is high enough or spurious mode loss is low enough that significant spurious mode power can be built up during one traversal and then be reconverted to the TE_{01} mode in the next

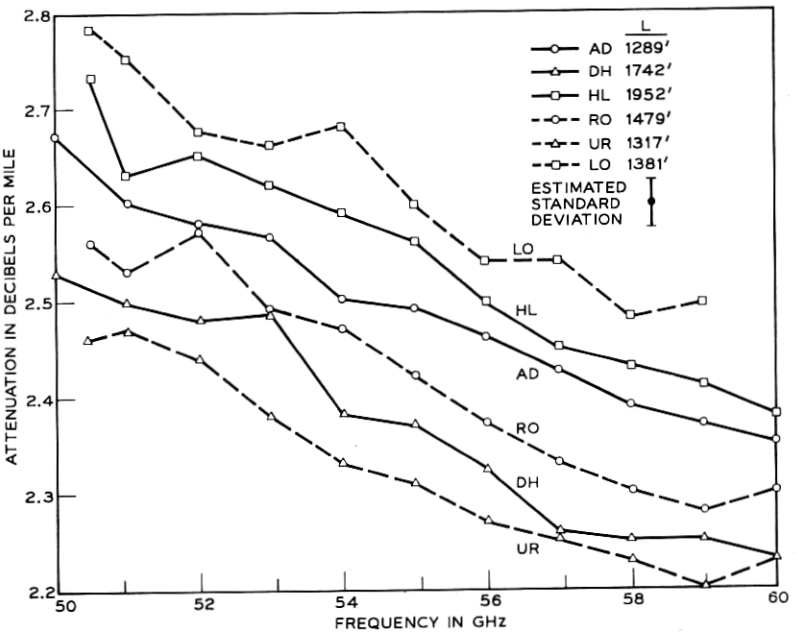

Fig. 4 — Measured attenuation of medium length waveguide sections.

traversal, and (*ii*) between nonsuccessive trips when the test section length L and the delay line length l are related by $mL \approx nl$ so that pulses bouncing in the delay line as a result of reflections or mode conversions at the input transducer can coincide with some of the desired signal pulses bouncing in the test section.

The first type of interaction is readily observed in waveguides with low spurious mode loss and has been discussed[4] in detail. The cure in the low-loss case is to provide mode filters at each end of the test section. For helix waveguide with high spurious mode loss, as in our experiments, it is expected that the spurious mode level is never high enough to cause observable interactions for all except TE_{0n} modes. This expectation was tested in several guide sections at several frequencies by using a movable shorting piston and observing the signal pulse after many round trips. By moving the shorting piston one changes the phases of any reflected spurious modes and thus of the reconverted TE_{01}, causing distinctive variations in the observed signal pulse height.[4] No variations outside experimental uncertainty were observed with the exception of a series of narrow loss peaks at the TE_{02} spacing.

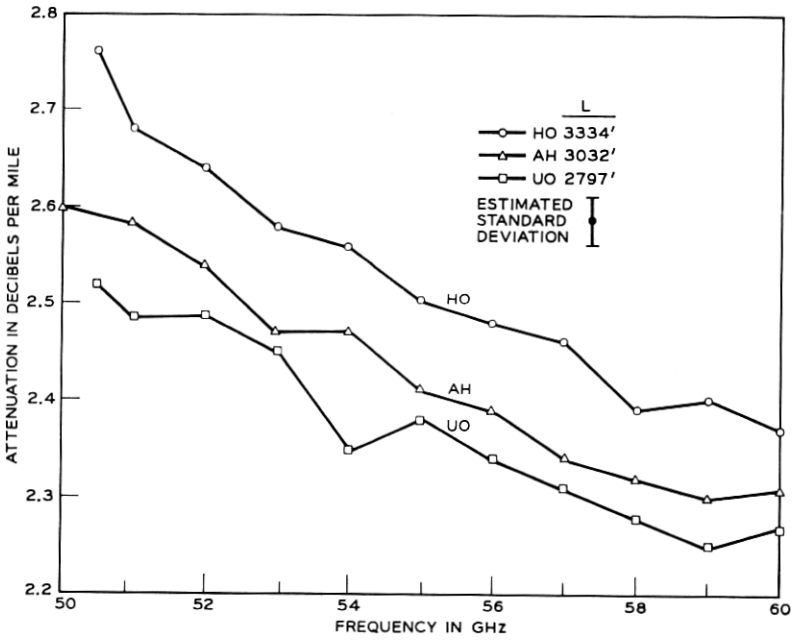

Fig. 5 — Measured attenuation of long length waveguide sections.

The TE_{02} mode is coupled to TE_{01} by imperfections possessing circular symmetry,[10] such as diameter changes or slight dishing of the mesh or end pistons. Its loss in helix waveguide is very low, so it can interact over several trips in short waveguide sections, causing loss peaks when the frequency and section length L are such that $2L$ contains an integral number of TE_{01}–TE_{02} beat-wavelengths, or

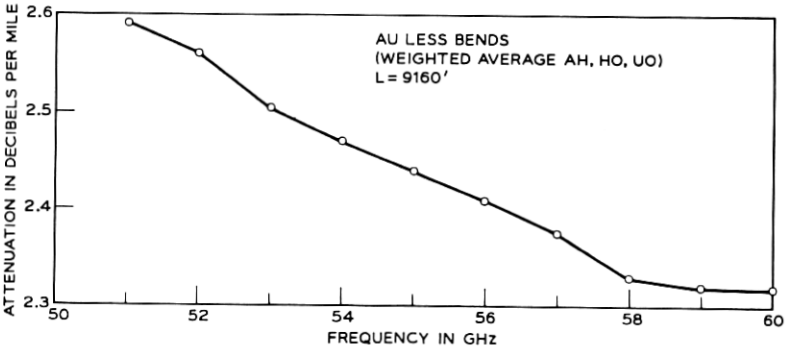

Fig. 6 — Measured attenuation of total straight waveguide.

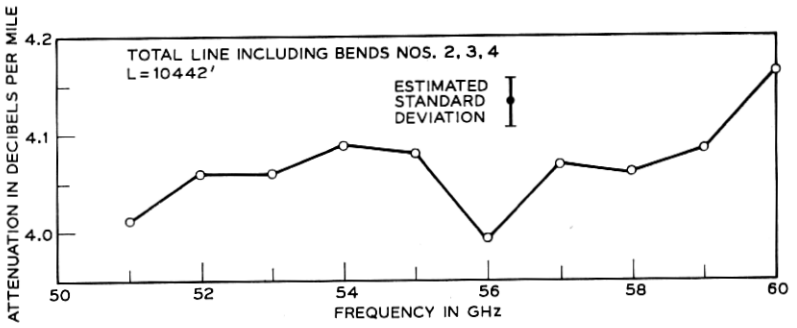

Fig. 7 — Measured attenuation of total line including bends.

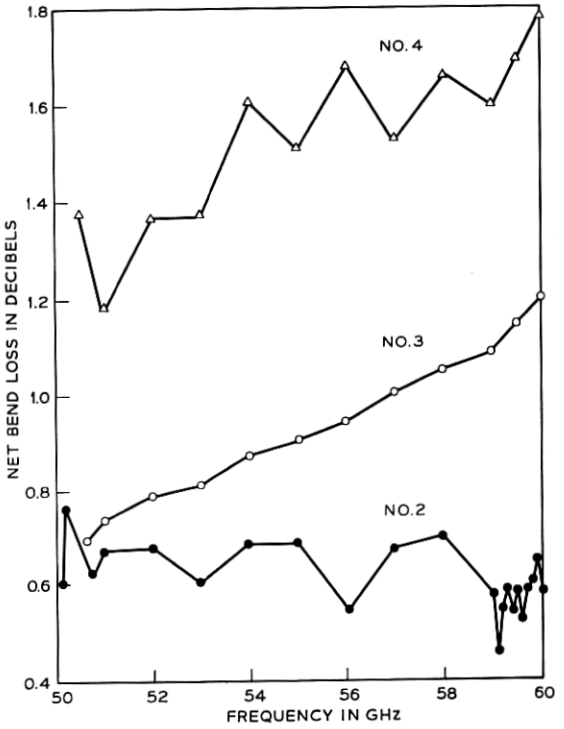

Fig. 8 — Bend losses.

nearly so.[4] The diameter tolerance of the helix waveguide was such that continuous conversion to TE_{02} was not expected to be observable, so conversion at the coupling mesh and end piston was suspected as the cause.

This suspicion was verified by the following experiment. The piston and mesh were fixed, and the test frequency was varied slowly. Loss peaks were observed every 120 MHz although the beat-wavelength condition was satisfied every 60 MHz in the test line. Such an effect should indeed occur if both mesh and piston are converters of roughly similar magnitude. When the coupling mesh was turned around, the loss peaks still occurred every 120 MHz but were shifted 60 MHz to frequencies between those observed originally, thus indicating the expected phase reversal in the coupling at the mesh. Various meshes and end-pistons were tried, with similar results.

It can be shown[5] that conversions 50 dB down at each end of the test section will cause 10 per cent additional loss at the loss-peak frequencies in a 450-foot section; to reduce this number significantly requires flatness beyond that obtainable with simple machining techniques. For our experiments, therefore, we selected the best mesh and piston available, and chose test frequencies which avoided the loss peaks. This precaution was unnecessary in sections 1500 feet or more long, as the extra peak loss was then below experimental uncertainty.

The second type of intertrip interaction was avoided by identifying and observing the spurious pulse trains arising from the delay line. Both TE_{01}, which is reflected for several trips with rapidly decreasing amplitude because of the mismatch at the transducer, and TE_{02}, which is generated at a low level in the taper to the transducer but is then almost totally reflected from taper and mesh on successive trips, are important. Certain test section-delay line combinations with nearly rational length ratios were not measured because these effects were observable. In general they become less important as the delay line length (and therefore its loss) increases.

A third possible cause of nonlinearity between pulse height and trip number is the receiver down-converter noise. This effect was observable only after many trips when the signal pulse was much attenuated and the receiver attenuator was set near zero; it was easily avoided by monitoring the signal-to-noise ratio.

Two other major sources of inaccuracy are oscillator stability and oxygen absorption. At one atmosphere pressure, contamination of the nitrogen filling gas by 0.02 percent of oxygen will increase the meas-

ured loss at 60 GHz by approximately 1 per cent. Thus the elaborate flushing procedures mentioned earlier were followed.

The oscillator frequency stability must be sufficient to hold the beating oscillator level at the receiver down-converter constant during a measurement run. The level will vary with frequency because the main return from the mesh at the end of the delay line will phase with the reflection from the transducer mismatch. In addition, the return from the mesh will change when the test line is in the vicinity of resonance for the beating oscillator frequency. These effects become severe as the lengths L and l become large. In the present experiments the BWO beam supply was regulated to a few millivolts, giving frequency stability of a few tens of kHz, but for lengths of either delay or test line of over 1000 feet it was necessary to monitor the converter crystal current very carefully to avoid serious loss of precision, and for lengths over 5,000 feet precise measurements became difficult.

IV. RESULTS AND COMPARISONS

4.1 *Individual Line Sections*

The measured attenuation constants vs frequency for several line sections are plotted in Figs. 3, 4, and 5, grouped roughly by length. The results for sections* AB, BC, CD, and DE, all of which are under 500 feet long, are plotted together in Fig. 3. Sections AD, DH, HL, LO, UR, and RO, from 1289 to 1952 feet long, are shown in Fig. 4. Results for the three long straight runs AH, HO and UO, all around 3000 feet long, are shown in Fig. 5. Notice that in all cases the vertical scales are greatly expanded.

On each figure is indicated the estimated standard deviation of the experimental points, $\langle(\alpha - \alpha_t)^2\rangle^{1/2}$, as calculated from equations (1) and (6). The actual value of this quantity of course varied somewhat from point to point and curve to curve; the indicated amount is a rough average. In general the actual value tended to be a bit larger at the lower frequencies in the band and smaller at the higher frequencies, because of the greater number of trips observable at lower attenuations.

The over-all high quality of the helix waveguide is evidenced by the low observed attenuation constants. The theoretical loss for per-

* The first letter in the section code refers to the manhole in which the coupling mesh was located and the second to the manhole with the piston. Manhole locations are indicated in Fig. 1.

feet solid-copper guide varies from 1.79 dB per mile at 50 GHz to 1.35 dB per mile at 60 GHz. Thus the additional losses from all causes, including finite helix-wire size and pitch, surface roughness, and manufacturing tolerances, total less than 1 dB per mile for most sections.

The rapid variations in loss vs frequency for each section are within the estimated experimental error in most cases. As mentioned earlier, in this waveguide we would expect to see no variations vs frequency with periods less than 6 GHz. None were observed, except the spurious TE_{02} peaks discussed in Section 3.3, and a peak at 54.3 GHz in line LO which is believed to be from a mechanical failure of the steel jacket-lossy lining bond in some of the helix waveguide pieces. Experiments over much wider frequency bands would be necessary to detect the very slow variations which are expected from the random curvature of the waveguide axis.

On the other hand, the difference in measured loss between one line section and another of roughly the same length is much greater than experimental error is most cases, and is therefore quite real. This difference is discussed in detail in Section 4.4, where it is compared with a theoretical estimate. It results from the statistical independence of the loss components between one section and the next; the variations vs frequency for a single section should be as great over frequency differences large enough that the statistical independence again holds.

Figure 6 shows the average attenuation constant for all of the horizontally straight line sections, obtained by adding the measured losses for sections AH, HO and UO and dividing by their total length. Figure 7 shows the average attenuation constant for the entire loop including sharp bends in the corner manholes. The mesh was in manhole A and the shorting piston in the laboratory building at the other end of the waveguide loop; thus everything was included except the short delay-line section between the building and A.

4.2 *Bend Losses*

The losses of several models of sharp bends for use in the corner manholes were measured by taking the difference between the losses of line sections with and without the bends included. The coupling mesh was placed in an appropriate manhole ahead of the corner manhole, and the shorting piston was placed in the corner manhole, first following the bend and then preceding it. In the measurement

with bend included, for nonhelix bends, a short section of helix waveguide was placed between the bend and the piston to serve as a mode filter.

The losses of bends 2, 3, and 4 are shown in Fig. 8. These bends were used in manholes H, O, and U, respectively, for the measurement shown in Fig. 7. Bend 2 is made of two 90° mitered elbows back to back, with a rotary joint between them adjusted to give the 42° horizontal angle. The measured loss agrees well with theory.[11] Bends 3 and 4 are 7/8 inch inside diameter helix waveguide with lossy jacket, bent 90° on elastically tapered curves, with effective bend radii of about 3 meters. The loss of bend 3 is in agreement with theory; that of bend 4 is considerably higher.

For all three bends the measurement accuracy is a few hundredths of one dB, thus the plotted variations vs frequency for bends 2 and 4 are real. For bend 2, some phasing between spurious modes generated at the two elbows is to be expected, but for bend 4 the variations further indicate that the helix waveguide was not properly constructed.

Figure 9 shows the measured attenuation of section XU, which contains the 708-foot radius horizontal bend. It also shows the predicted straight loss of XU, obtained by subtracting the calculated

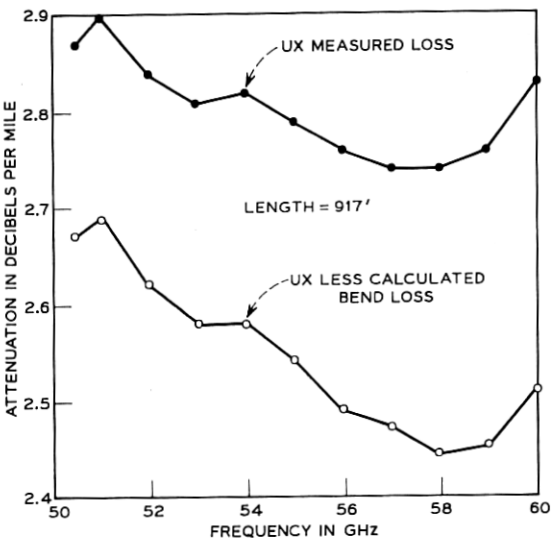

Fig. 9 — Added loss caused by large radius of curvature bend.

bend loss from the measured loss. The agreement with the measured losses for other straight sections as shown in Figs. 3 through 6, indicates that the effect of the horizontal bend is well predicted by theory.

4.3 *Sums of Sections and Residual Errors*

An important purpose of these experiments was to determine whether the sum of the losses of several sections measured individually would be the same as the loss measured for a line made up of the same sections connected. The assumption that this is indeed true is inherent in all predictions of the losses of long lines based on measurements on short lines. It is also inherent in our technique for measuring bends, and it underlies our assumption of the validity of the shuttle-pulse technique in general. Thus, although there were no known reasons to expect the assumption to be false, an experimental verification was considered important.

Figure 10 shows the difference in dB between the measured loss of section AD and the sum of the measured losses of sections AB, BC, and CD, as a function of frequency. The differences are very small indeed. The dashed lines indicate the average across frequency of the estimated standard deviation of the differences about zero as calculated from the sum of the mean square errors of the individual measurements as given by (6). The dashed lines thus indicate only the effect of the scatter of the data points and do not include any effects such as long-term drift of the apparatus between measurements, variations in oxygen contamination between sections, residual tails of the spurious TE_{02} loss peaks, or absolute errors such as in the end correction due to mesh and piston.

The scatter in Fig. 10 of the experimental differences is therefore

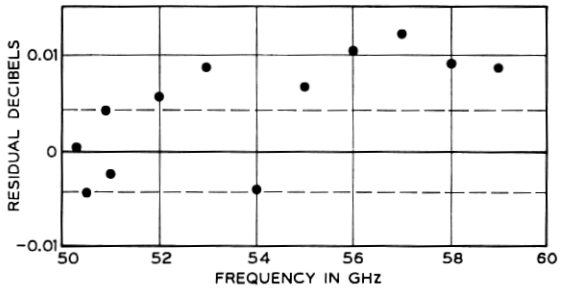

Fig. 10 — Residual dB for difference AD—(AB+BC+CD). The dashed lines are the estimated standard deviations about zero owing to measurement variations only.

quite satisfactory. The measured loss of section AD is about 0.6 dB and of its shorter component sections about 0.2 dB; the largest observed difference is thus just 2 per cent of the loss of AD, and about half of the observed differences are within 1 per cent. All of the differences would be shifted a constant 0.004 dB, or 2/3 per cent of the loss of AD, by a fixed absolute error of 0.002 dB in all measurements. That amount is roughly the limit of accuracy of the measurement of the mesh and piston end correction. In addition, oxygen contamination would cause an error rising from zero at 50 GHz to 1 per cent at 60 GHz in any section with 0.02 per cent oxygen from improper flushing or filling.

The addition of longer sections, where the end correction is unimportant, is shown in Fig. 11. Here the difference is between the loss of section AO and the sum of the losses of sections AH and HO and of bend 2. Bend 2 was itself measured by taking the difference of the losses of section GH with and without the bend included. The dashed lines are again the estimated standard deviation about zero as calculated from data point scatter only. The loss of section AO is about 3.6 dB, so the dashed lines are at slightly over ± 1 per cent. The experimental points fall quite satisfactorily within them.

Other additions were checked with similar results. The direct measurements made during these experiments are thus believed to be accurate to the order of about ± 1 per cent or ± 0.005 dB, whichever is greater, and the sums of losses of individual sections are the same as the loss of the sum of the sections to within that measurement accuracy.

4.4 *Statistical Confidence Limits*

A further purpose of these experiments was to determine experimentally the variation in attenuation between different waveguide sections and to try to discover the length of guide that must be

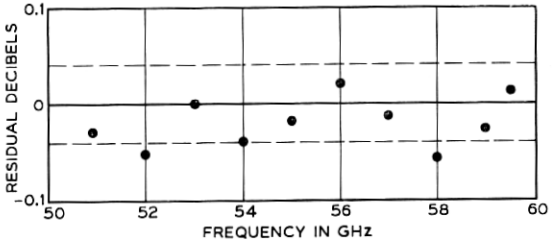

Fig. 11 — Residual dB for difference AO—(AH+HO+bend 2).

measured in order to obtain estimates of a given accuracy on the loss of very long waveguide runs. We assume that the loss variations among sections are caused by variations in the mode conversion in the different sections and are thus determined by a random process whose statistics are related to the statistics of the mechanical tolerances of the guide.[4, 5]

A theoretical solution for the confidence limits on loss as a function of sample length requires knowledge of the probability function for the additional loss caused by mode conversion. An exact solution is difficult when the differential loss between coupled modes is nonzero. An approximate solution for two modes and two polarizations is given in the Appendix; it predicts a normal distribution with mean unity and variance $1/(4 \mid \Delta\alpha \mid L)$ for the quantity $A/\langle A\rangle$. Here A is the additional loss caused by mode conversion and is thus the difference between actual loss and theoretical heat loss. $\langle A\rangle$ is its expected value.

In Fig. 12 the $\pm 2\sigma$ lines for the predicted theoretical distribution are plotted as a function of line length along with experimental values of $A/\langle A\rangle$ for all line sections measured. The experimental value of $\langle A\rangle$ was derived from the curve shown in Fig. 6, so is itself subject to experimental error. The values of $A/\langle A\rangle$ plotted for each line are the means of the maximum and minimum values observed vs frequency.

The fit between theory and experiment would be better if the plotted curves were at $\pm 1\sigma$ instead of $\pm 2\sigma$. However, the approximations of the theory, which includes only one spurious mode, and the experimental accuracies of the points are probably sufficient causes for the poor agreement. In addition the manufacturing variations in our virtually hand-made waveguide may be considerable. It should be remembered that

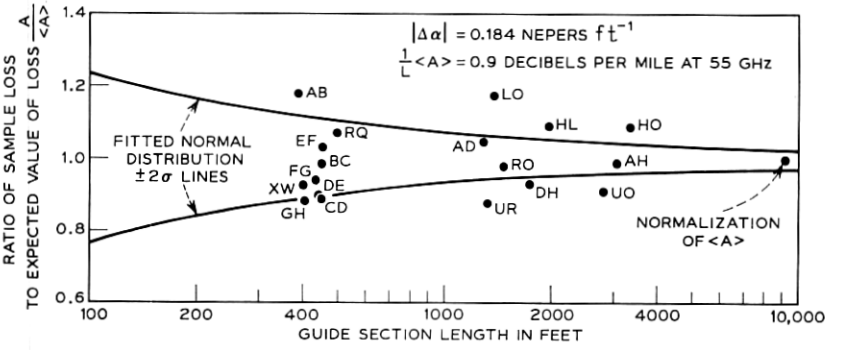

Fig. 12 — Theoretical confidence limits for measurements vs length of waveguide.

the quantity A is the additional loss only, and the value of $\langle A \rangle / L$ is less than one dB per mile. Thus less than 4 per cent variation in the observed total loss will cause a 10 per cent variation in A. The experimental errors are similarly magnified.

Assuming that the theoretically predicted variance of A is correct, one needs to measure 2000 feet of our present waveguide to assure 95 per cent confidence that the measurement is within 5 per cent of the true value of A or thus within 2 per cent of the true value of attenuation constant α. Two per cent gives the loss of a 20-mile section to ± 1 dB. If the variance were twice that predicted, one would need to measure four times as much guide, or 8000 feet, for the same confidence.

V. SUMMARY

Precise measurements have been made across the 50 GHz to 60 GHz band on many sections of a two-mile long loop of two-inch inside diameter helix waveguide. The measurement accuracy is approximately ± 1 per cent or ± 0.005 dB, whichever is greater.

The waveguide is of high quality; the average measured attenuation varies smoothly from 2.62 dB per mile at 50 GHz to 2.32 dB per mile at 60 GHz. Fast variations vs frequency were within experimental error.

The losses of several long sections were compared with the sum of the losses of the smaller sections of which they were composed; the agreement was excellent and within experimental error. Several short-radius bends of different angles were included in the line and measured; losses less than 0.8 dB across the band were observed for a 42° bend made of two mitered elbows.

Differences among line sections in the values of their measured losses were considerably greater than variations vs frequency for any one section, as was expected. It was found that quantities of waveguide from 2000 to 8000 feet must be measured in order to be 95 per cent assured that the measurement is typical of the population to within 2 per cent.

APPENDIX

Approximate Confidence Limits for the Variations Between Guide Sections

For the case of one spurious mode with nonzero differential loss $\Delta\alpha$, Young has shown[9] that the additional loss in a guide of length

L is given by convolving the expression for the additional loss when $\Delta\alpha = 0$ with a particular loss function. Thus

$$A(t) = \int_{-\infty}^{\infty} B(t - s)A_0(s)\, ds, \tag{7}$$

where $A_0(t)$ is the additional loss if $\Delta\alpha = 0$, and where B is the function,

$$B(t) = \frac{2}{|\Delta\alpha|} \frac{1}{1 + \left(\frac{2\pi}{\Delta\alpha} t\right)^2}. \tag{8}$$

The variable t is most conveniently taken as $t = \Delta\beta/2\pi$, where $\Delta\beta$ is the differential phase constant between signal and spurious modes. t is thus roughly proportional to the wavelength λ. The function A_0 has been extensively studied by Rowe and Warters,[5] who show that under reasonable restrictions it is a band-limited function and can thus be expressed by its values at its sample points, which are spaced by

$$\Delta t = \frac{1}{2L}. \tag{9}$$

If the convolution function B is much broader than Δt, meaning that $|\pi/\Delta\alpha L| \ll 1$, we can approximate A_0 by constant line segments through its sample-point values, and can estimate the convolution integral (7) as a summation over the sample points. This gives

$$A(t) = \sum_{i=-\infty}^{\infty} B(t - s_i)A_0(s_i)\, \Delta s \tag{10}$$

where

$$s_i = \Delta\beta_i/2\pi = i/2L.$$

Thus

$$A\left(\frac{\Delta\beta}{2\pi}\right) = \frac{1}{|\Delta\alpha L|} \sum_{i=-\infty}^{\infty} \frac{A_0(s_i)}{1 + \left(\frac{\Delta\beta L - i\pi}{\Delta\alpha L}\right)^2}. \tag{11}$$

For convenience we study $A(\Delta\beta/2\pi)$ at the Nth sample-point $(\Delta\beta_N)/2\pi = N/2L$. After substituting $n = N - i$ in the summation, we have

$$A\left(\frac{\Delta\beta_N}{2\pi}\right) = \frac{1}{|\Delta\alpha L|} \sum_{n=-\infty}^{\infty} \frac{A_0(s_{N-n})}{1 + \left(\frac{n}{n_0}\right)^2}, \tag{12}$$

where

$$n_0 = \frac{\Delta\alpha L}{\pi}.$$

From our earlier requirement on the width of the loss function B, we require $n_0 \gg 1$.

If the coupling coefficient between signal and spurious mode is expressed as a complex Fourier series for the length L, the additional loss A_0 is simply expressed in terms of the Fourier coefficients.[5] For two polarizations of the spurious mode,

$$A_0(t) = \frac{1}{2}\sum_{k=1}^{4} I_k^2(t), \tag{13}$$

where

$$I_k(t) = L\sum_{n=-\infty}^{\infty} K_{kn}(-1)^n \frac{\sin \pi(t-n)}{\pi(t-n)}. \tag{14}$$

The index n denotes the nth Fourier coefficient; the index k separates the real and imaginary parts of the coefficients for the two polarizations and thus has four possible values. If the x and y components of the mechanical imperfections are independent random Gaussian variables with white power spectrum, then so are the K_{kn}, at least for large L and over small percentage bandwidths.[5] Under these assumptions one finds that

$$\langle A_0(t_N)\rangle = 2L^2\langle K_N^2\rangle = 2L^2\langle K^2\rangle \tag{15}$$

and

$$\begin{aligned}\langle A_0(t_N)A_0(t_M)\rangle &= 6L^4\langle K^2\rangle^2, \qquad M = N\\ &\approx 4L^4\langle K^2\rangle^2, \qquad M \neq N.\end{aligned} \tag{16}$$

Expressions (15) and (16) are then used to calculate the lower-order statistics of the loss function A from (12), giving

$$\langle A(t_N)\rangle = 2L^2\langle K^2\rangle = \langle A_0(t_N)\rangle \tag{17}$$

$$\begin{aligned}\langle \delta A^2(t_N)\rangle &\equiv \langle (A - \langle A\rangle)^2\rangle\\ &\approx \frac{\langle A_0(t_N)\rangle^2}{4\mid \Delta\alpha L\mid}.\end{aligned} \tag{18}$$

The requirement $\mid \Delta\alpha L \mid \gg \pi$ has been used to simplify the expressions.

Since A_0 is a sum of squares of samples from a Gaussian process,

and since A is a weighted sum of values of A_o, it seems reasonable that the distribution function for A should be close to a chi-squared distribution with appropriate normalization. However, for large $\Delta\alpha L$ the approximate chi-squared distribution will have many degrees of freedom, approaching a normal distribution. Therefore, for large $\Delta\alpha$ the variable $A/\langle A\rangle$ becomes normally distributed, with unit mean and variance $1/(4 \mid \Delta\alpha L \mid)$. For this distribution the 95 per cent confidence limits are the $\pm 2\sigma$ lines.

$$\left.\frac{A}{\langle A\rangle}\right|_{\pm 2\sigma} = 1 \pm \frac{1}{\mid \Delta\alpha L \mid^{\frac{1}{2}}}. \tag{19}$$

The lines are plotted, together with the experimental observations on various waveguide sections of different lengths, in Fig. 12. The value of $\Delta\alpha$ used is -0.184 neper per foot, which is typical of the differential TE_{12} loss in lossy-jacketed helix waveguide. For sections with L greater than 300 feet, $\mid \Delta\alpha L \mid$ is greater than 55, so the approximation $\mid \Delta\alpha L \mid \gg \pi$ is well satisfied.

REFERENCES

1. Miller, S. E., "Waveguide as a Communication Medium," B.S.T.J., *33,* No. 6 (November 1954), pp. 1209–1266.
2. Unger, H. G., "Helix Waveguide Theory and Applications," B.S.T.J., *37,* No. 6 (November 1958), pp. 1599–1647.

2B. Unger, H. G., "Helix Waveguide Design," Proc. IEE, *106,* Part B, Suppl. 13 (September 1959), pp. 151–155.

3. Beck, A. C. and Rose, C. F. P., "Waveguide for Circular Electric Mode Transmission," Proc. IEE *106,* Part B, Suppl. B (September 1959), pp. 159–162.
4. Rowe, H. E. and Warters, W. D., "Transmission Deviations in Waveguide Due to Mode Conversion: Theory and Experiment," Proc. IEE *106,* Part B, Suppl. 13 (September 1959), pp. 30–36.
5. Rowe, H. E. and Warters, W. D., "Transmission in Multimode Waveguide with Random Imperfections," B.S.T.J., *41,* No. 3 (May 1962), pp. 1031–1170.
6. King, A. P. and Mandeville, G. D., "The Observed 33 to 90 kMc Attenuation of Two-inch Improved Waveguide," B.S.T.J., *40,* No. 5 (September 1961), pp. 1323–1330.
7. Steier, W. H., "The Attenuation of the Holmdel Helix Waveguide in the 100–125 kMc Band," B.S.T.J., *44,* No. 5 (May–June 1965), pp. 899–906.
8. Hoel, P. G., *Introduction to Mathematical Statistics,* New York: Wiley, 1947.
9. Young, D. T., "The Effect of Differential Loss on Approximate Solutions to the Coupled Line Equations," B.S.T.J., *42,* No. 6 (November 1963), pp. 2787–2793.
10. Morgan, S. P., "Mode Conversion Losses in Transmission of Circular Electric Waves Through Slightly Noncylindrical Guides," J. Appl. Phys. *21* (April 1950), pp. 329–338.
11. Marcatili, E. A. J., "Miter Elbow for Circular Electric Mode," Symposium on Quasi-Optics, Polytechnic Institute of Brooklyn (June 1964), pp. 535–542.